ELSEVIER

Advances in Colloid and Interface Science 108–109 (2004) 287–301

ADVANCES IN COLLOID AND INTERFACE SCIENCE

www.elsevier.com/locate/cis

Maximum bubble pressure tensiometry—an analysis of experimental constraints

V.B. Fainerman[a], R. Miller[b,*]

[a]*Medical Physicochemical Centre, Donetsk Medical University, 16 Ilych Avenue, Donetsk 83003, Ukraine*
[b]*Max-Planck-Institut für Kolloid und Grenzflächenforschung, Forschungscampus Golm, 14476 Potsdam/Golm, Germany*

Abstract

The maximum bubble pressure tensiometry is the only technique that allows measurements of dynamic surface tensions of surfactant solutions in the short time range down to milliseconds and even below. To reach such extremely short adsorption times, many hydrodynamic and aerodynamic effects have to be taken into consideration in order to measure physical values or to correct for the respective influences. In particular, the design of the instruments, and essentially the geometry of the measuring cell and capillary, are of key importance for accurate experiments. Another important issue is the way of determination of the characteristic bubble times, such as bubble dead time and lifetime. Examples demonstrate that the bubble pressure technique provides a powerful tool for studies of adsorption dynamics even for solutions of higher viscosities.

Keywords: Maximum bubble pressure tensiometry; Surfactant solutions; Dynamic surface tensions; Short adsorption times; Dead time determination

1. Introduction

Already 150 years ago the maximum bubble pressure method (MBPM) was proposed by Simon [1] for measuring the surface tension of liquids. In recent reviews the various aspects of this method were discussed [2–7]. The physical processes taking place during the growth and separation of a bubble from the tip of a capillary, the problems of measuring bubble pressure, lifetime and so-called dead time were considered in many papers [7–30]. Using this method, significant results have been obtained in many fields of application where dynamic surface tensions at short adsorption times are required, including industrial and biological applications [31–50].

The successful development of theory and technique of the MBPM are the reason why today various types of bubble pressure tensiometers are commercially available: Sensadyn 5000 (Chem Dyne Research Corp., USA), BP2 (Krüss, Germany), T60 (SITA Messtechnik GmbH, Germany), MPT2 (Lauda, Germany) and BPA-1 (SINTERFACE, Germany). The main reasons are the possibility of automation of measurement and calculation procedures, and in particular the increasing demand for studies of dynamic surface phenomena at very short times. In these tensiometers, capillaries of different size are used. Also, the technical principles employed for measuring the surface lifetime are different. This leads to dynamic surface tensions that deviate significantly from each other when measured with different instruments [51].

In some instruments, the surface tension is directly determined from the maximum pressure in the instrument's gas system connected to the capillary. The lifetime of the bubble (t_l) and the dead time (t_d) are estimated from the change in the measured pressure: t_l from the increasing part and t_d from the decreasing part of the pressure curve. This procedure is self-contradictory: precise measurements of surface tension based on the pressure in the system require a system volume much larger than the volume of a single separating bubble [2,7,30]. At the same time, precise measurements of the lifetime can be performed only if the system volume is relatively small. We will show below that the attempt to minimise the error (say, to keep within 1%) for one of the measured parameters results in a significant increase in the error for other parameters: for

*Corresponding author. Tel.: +49-331-567-9252; fax: +49-331-567-9202.
E-mail address: miller@mpikg-golm.mpg.de (R. Miller).

0001-8686/04/$ - see front matter © 2004 Elsevier B.V. All rights reserved.
doi:10.1016/j.cis.2003.10.010

surface tension the error becomes 3–10%, while for the lifetime this error can amount up to 50% of the determined value.

In the tensiometers MPT2 (LAUDA) and BPA (SINTERFACE), the precision of surface tension measurements is high due to the large volume of the measurement system (up to 40 ml). The procedure employed for the determination of the lifetime in the MPT2 was described earlier [2,18,29]: first, the critical pressure (or critical flow rate) is localised in the pressure–flow rate curve $P(L)$. The interval between bubbles in the point of critical flow rate (the transition point between the bubble and jet regimes) is measured. This time interval is equal to the dead time, which for any arbitrary flow rate can be recalculated via the measured pressure using the Poiseuille law. This method has the drawback that the consideration of hydrodynamic effects in the calculation of dead time and lifetime is quite cumbersome [7,25–28]. Also, the implementation of the method requires preliminary measurement of the entire pressure–flow rate characteristic and determination of the critical point, which restricts the applicability of the method and makes it rather slow.

In a recent paper [52] an essentially new method for the measurement of the surface lifetime was proposed, which is free of the deficiencies mentioned above. The method employs explicit measurements of the dead time and lifetime from the oscillations of the gas flow from the measurement system to the capillary. This is in contrast to other tensiometers where the pressure signal is directly used. The method is based on the fact that during the period of lifetime the air flow from the measuring system to the capillary is very small, and finally the growth of the bubble becomes almost zero. During period of rapid bubble growth and final separation from the capillary, the so-called dead time, the air flow from the measuring system to the capillary, increases strongly and attains its maximum in the moment of separation. Therefore, the air flow from the external system to the measuring system oscillates and can be used to measure the interval between two bubbles and to exactly determine the bubble dead time and lifetime. In contrast to the method where the t_1 values are measured from pressure oscillations, as known from the BP2 and SITA tensiometers, this new method does not require a small volume of the measuring system, so additional errors in the surface tension measurement do not arise.

The present manuscript gives an overview of the main experimental aspects of bubble pressure tensiometry, not only in respect to the measurement of characteristic times of bubble formation. An analysis of the influence of the geometry of the measurement system, and the design of the capillary on the measured surface tension data, is given. A comparison of results obtained demonstrates how large results from measurements with different instruments can deviate.

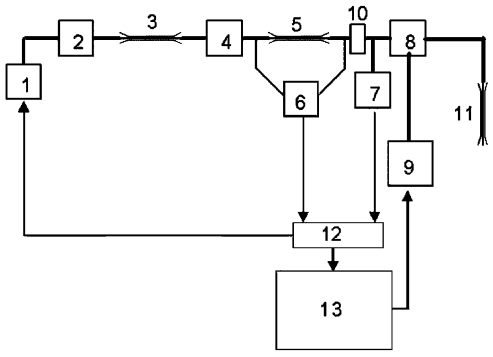

Fig. 1. Schematic diagram of a maximum bubble pressure tensiometer with a gas flow oscillation analyser (BPA); (1) pump or compressor, (2, 4) pneumatic volume, (3, 5) capillaries, (6) differential pressure sensor, (7) pressure sensor, (8) internal gas volume of the instrument, (9) Peltier block, (10) valve, (11) measuring capillary, (12) interface PC-instrument, (13) computer.

2. Typical scheme of a tensiometer, measuring procedure and data analysis

The designs of bubble pressure tensiometers are various. As an example, Fig. 1 illustrates the flow chart of the tensiometer BPA (SINTERFACE). It is equipped with a gas flow oscillation analyser, in which the above mentioned new method for the determination of bubble surface lifetime is implemented. One important peculiarity is, for example, the pneumatic system. The air or any other gas is pressed by the compressor 1 through the gas volume 2, capillary 3 and gas volume 4, which smoothen the flow and pressure at the inlet of the measuring system. The air flow is determined from the pressure difference along the flow capillary 5 via a differential pressure sensor 6. The control of the volume of separating bubbles is arranged by a deflector located opposite to the capillary at a definite distance [18]. The optimum internal gas volume of the instrument 8 and selection of the right capillary are two important points in the design of the device and will be discussed in detail below.

The measurement procedure is usually quite simple—the pressure is measured as a function of bubble rate and further analysed depending on the algorithms implemented in the respective instrument. The BPA discussed here has a more complex procedure that finally makes it suitable for measurements at very short adsorption times [53]. The pressure in the internal volume P_s and the gas flow rate L are measured as a function of time and recorded in 0.5-ms intervals. Note that in the MPT2 only the average gas flow L is registered. In Figs. 2 and 3, examples of dependences $L(t)$ and $P_i(t)$ are shown. Arrows indicate the various phases of bubble growth.

The time intervals between successive maxima or minima in P_s and L constitute the total bubble time necessary for the formation and separation of each bubble: $t_b = t_l + t_d$. The duration of the increase in L (Fig. 2) and decrease in P_s (Fig. 3), respectively, corresponds to the dead time t_d. To calculate the lifetime t_l, two methods can be used. At first it can be calculated from the relation $t_l = t_b - t_d$ with t_b and t_d determined as explained above. Secondly, we can obtain it from the time intervals of decrease in L and increase in P_s, respectively. After averaging the t_l obtained values, the results of the two methods are compared and the value with the lower standard deviation is accepted.

The maximum pressure in the measuring system is calculated from the peaks in the dependence $P_s(t)$ (cf. Fig. 3) also averaged over a certain number of measured oscillations (10–400 cycles, depending on the given bubble formation frequency). The surface tension γ can be calculated from the measured maximum capillary pressure P and the known capillary radius r using the Laplace equation

$$\gamma = f\frac{r \cdot P}{2}. \quad (1)$$

The correction factor f is needed for capillaries with a radius $r > 0.1$ mm, which is the case for all commercial instruments. For capillaries of small radii (≈ 0.1 mm) the bubbles are sufficiently spherical and the error of calculation of γ from Eq. (1) with $f = 1$ is less than 0.5%. Thus, a calibration with a known liquid eliminates this error completely. For wide capillaries, for example 1 mm, as used in some tensiometers [54,55], the error in the surface tension of water can amount up to 10% [35]. When surfactant solutions are studied, this error increases and is roughly proportional to the ratio between the surface tensions of water and this surfactant solution. This means that for surfactant solutions a calibration with respect to water does not work and errors of 10% and more can arise. Note that all known corrections are valid under static conditions. The fast bubble formation is a highly dynamic process and the error arising from Eq. (1) is even higher, caused by dynamic effects. Especially for surfactant solutions this leads to increase radii of the growing bubbles [7,28,30].

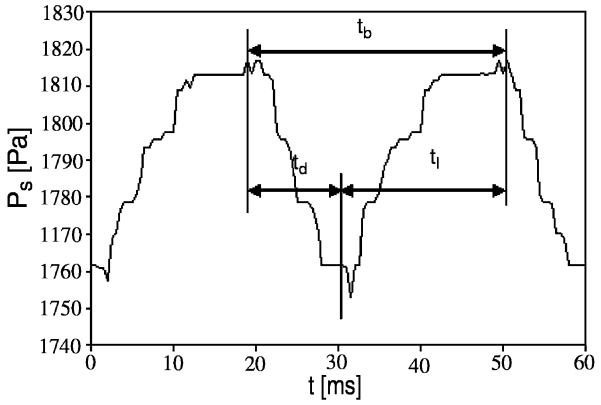

Fig. 3. The example of the $P_s(t)$ dependence. Arrows indicate the duration of corresponding stages of bubble growth.

The measured capillary pressure P can be expressed via the excess maximum pressure in the measuring system P_s, the hydrostatic liquid pressure $P_H = \Delta\rho g H$ and the excess pressure P_d (arising due to dynamic effects, such as aerodynamic resistance of the capillary and viscous of the liquid, etc.), while $\Delta\rho$ is the difference between the densities of liquid and gas, g the gravity and H the immersion depth of the capillary into the liquid. Hence, the capillary pressure is given by [2,7]

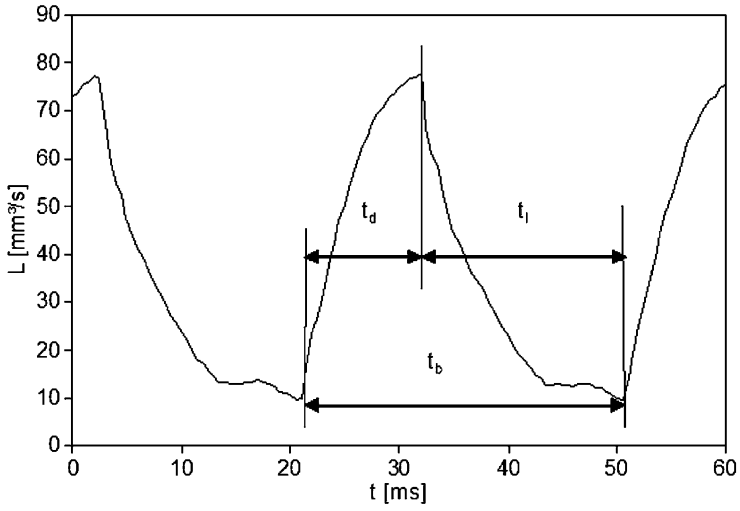

Fig. 2. The example of the $L(t)$ dependence. Arrows indicate the duration of corresponding stages of bubble growth.

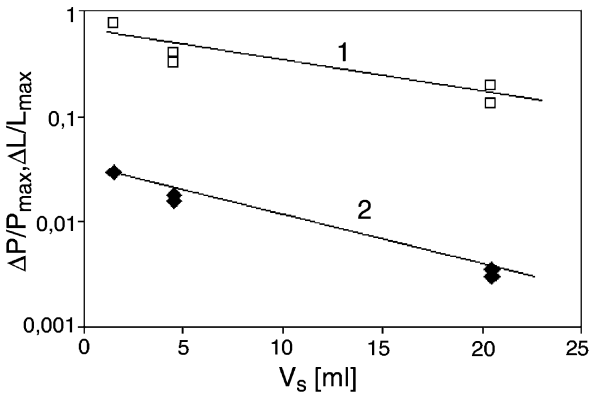

Fig. 4. The dependence of $\Delta L/L_{max}$ (curve 1) and $\Delta P/P_{max}$ (curve 2) on V_s.

$$P = P_s - P_H - P_d, \tag{2}$$

and from Eqs. (1) and (2) we have

$$\gamma = f\frac{r(P_s - P_H)}{2} - \Delta\gamma_a - \Delta\gamma_v \tag{3}$$

The term $\Delta\gamma_a$ represents the effect caused by the aerodynamic resistance, and the second additional term $\Delta\gamma_v$ reflects the effect of viscosity of the studied liquid.

3. Analysis of experimental data

3.1. Comparison of two methods for the determination of the bubble lifetime

In the experiments given in Ref. [52] a capillary of radius 0.085 mm and length approximately 10 mm was used, and the deflector was located in a distance of 1 mm from the capillary tip. As mentioned above, the deflector ensures the formation of separating bubbles with constant volume almost independent of the frequency. In the mentioned experiments, system volumes of $V_s = 1.5$, 4.5 and 20.5 ml, respectively, were used. For a bubble volume of $V_b = 2$ mm^3, ratios of $V_s/V_b =$ 750, 2.250 and 10.250, respectively, result.

Dependencies of the relative change of air flow $\Delta L/L_{max}$ and pressure $\Delta P/P_{max}$ in the measuring system on the system volume V_s are shown in Fig. 4. Here ΔL and ΔP are differences between the maxima and minima of the air flow L and pressure P, respectively (cf. Figs. 2 and 3). Figs. 5 and 6 illustrate the dependencies $L(t)$ and $P_s(t)$ for water at similar t_l values for a system volume $V_s = 20.5$ ml. The analysis of the dependencies

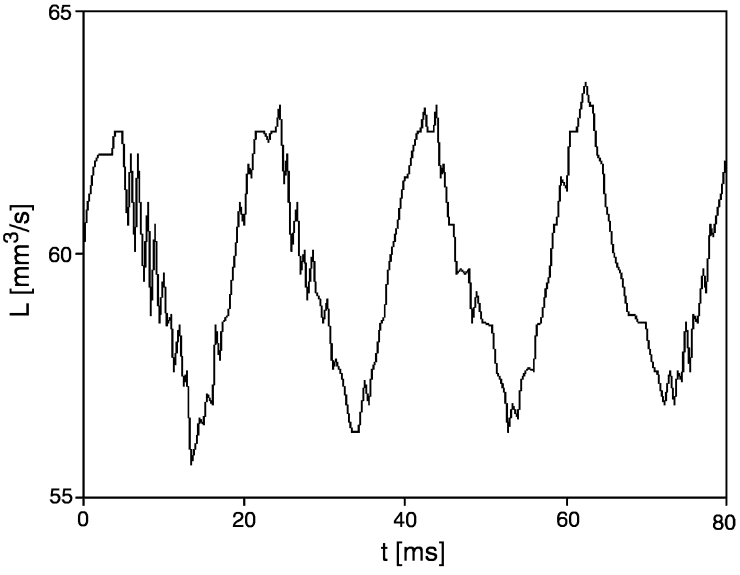

Fig. 5. The $L(t)$ dependence for a system volume of 20.5 ml.

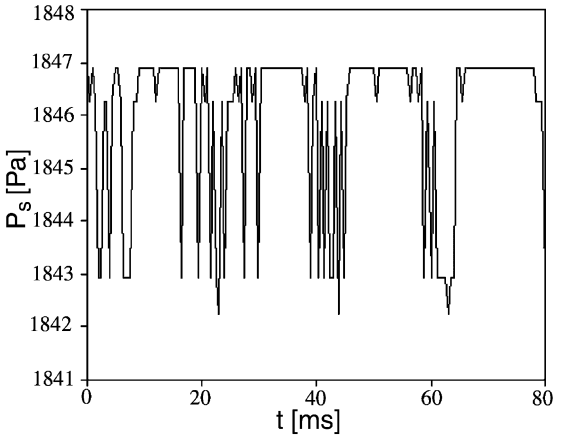

Fig. 6. The $P_s(t)$ dependence for a system volume of 20.5 ml.

shown in Figs. 4–6 yields a number of significant differences:

i. the relative amplitude of measured flow oscillations is more than one order of magnitude higher than the relative amplitude of system pressure oscillations;
ii. the values of t_l and t_d can be precisely determined from the flow oscillations irrespective of the measuring system volume;
iii. the bubble lifetime can be accurately determined from pressure oscillations only for a minimum system volume;
iv. for $V_s = 4.5$ and 20.5 ml the onsets of pressure decrease and increase are unclear (Fig. 6), and this uncertainty is comparable with the value of t_d.

The expected pressure decrease in the measuring system due to the growth and separation of a bubble during the dead time interval can be estimated from the expression [7]

$$\Delta P_s/P_s = (P_{max} - P_{min})_s/P_s \cong \frac{V_b}{V_s}\frac{P_a + P_s}{P_s}, \quad (4)$$

As the excess pressure in the system P_s is small as compared to the atmospheric pressure P_a, one can take only the atmospheric pressure $P_a = 10^5$ Pa for estimates with Eq. (4). For example, for the compared system volumes the obtained $\Delta P_s/P_s$ values are 0.048, 0.016 and 0.004, respectively, which are quite close to the experimental values shown in Fig. 4.

Note that the results discussed here were obtained for narrow capillaries. For wider capillaries (with radius $r_{cap} \geqslant 0.5$ mm), and small measuring system volumes (as it is the case, for example, in the SITA tensiometer [54,55]), the course of pressure minima in the $P_s(t)$ curve is different. In this case, the growth of the bubble during the dead time leads to a significant drop of the excess pressure in the system so that for large separating bubbles the pressure minima can be comparable to the hydrostatic pressure at the bubble tip. For conditions of the SITA tensiometer the ΔP_s difference is relatively high (close to P_{max}), due to the very low capillary pressure and the low ratio V_s/V_b. It will be shown below that a small ratio V_s/V_b alone causes large errors in the measured maximum pressure, which finally leads to large errors in the surface tension of surfactant solutions. P_{min} cannot be lower than the hydrostatic pressure, otherwise a formation and separation of bubbles were impossible. Thus, for large separating bubbles and a small ratio V_s/V_b we can get $P_{min} \approx P_H$. In this case, however, the separation of a bubble is followed by a penetration of liquid into the capillary even when the internal surface of the capillary is hydrophobized [7,29]. This fact, in addition to the necessary account for the non-spherical bubble shape in Eq. (1), makes an analysis of such tensiometry data in the framework of common theoretical adsorption models quite cumbersome [2,29].

When we compare the standard measurement errors for the time values measured by the two methods, we can see that the absolute measurement error for the determination of t_l and t_d from flow oscillations in the range between 5 and 20 ms does not exceed 1 ms (i.e. is close to the instrumental error) and is independent of the measuring system volume. In contrast, the calculations based on pressure oscillations for the system with minimum volume (1.5 cm^3) have a standard error in the determined t_l values of 1.5–3 ms, for $V_s = 4.5$ cm^3 the standard error is 4–5 ms and for $V_s = 20.5$ cm^3 the standard error becomes as high as 10 ms. Therefore, the measurement of bubble lifetimes based on pressure oscillations is possible only for very small system volumes, while for larger volumes this method becomes unacceptable for surface lifetimes in the range of milliseconds. The absolute standard error in the determination of t_l from flow oscillations at $t_l > 20$ ms becomes higher because of certain instabilities in the bubble generation process; however, the relative standard error in the range from 20 to 1000 ms does not exceed 4%.

The advantages of the proposed method of determining the surface lifetime are more evident when data for surfactant solutions are considered. In Ref. [52], solutions of dodecyl phosphine oxide (C_{12}DMPO) at a concentration of 1 mmol/l at 20 °C were measured. Similarly to the results obtained for water, the detection based on gas flow oscillation provides an unambiguous differentiation between all phases of bubble formation. On the other hand, the same differentiation from pressure oscillations becomes doubtful even for $V_s = 4.5$ cm^3. For the largest system volume $V_s = 20.5$ cm^3, the differentiation between different phases of bubble formation becomes impossible, and only the bubble time t_b can be determined.

3.2. Determination of the so-called dead time

Fig. 7 illustrates measurements of bubble time $t_b = t_d + t_l$ and dead time t_d using the flow oscillation method [53] for water and a C_{12}DMPO solution with measurement systems of different gas volume. For a given liquid, the dependence $t_d(t_b)$ is almost independent of V_s, which is in agreement with the maximum bubble pressure theory and indicates that the use of the deflector is justified [2]. The deflector ensures a stabile bubble size irrespective of the formation frequency, and, therefore, the dead time remains approximately constant at a fixed system pressure P_s. This is seen to be true for the data for water as shown in Fig. 7. The variation of P_s due to the variation in the surface tension of the surfactant solution or additional dynamic effects in the short time range is taken into account via the Poiseuille equation [2,18]. The two lines 1 and 2 were calculated

from the system pressure according to the relationship

$$t_d = t_d^* \frac{P_s^*}{P_s}, \quad (5)$$

where asterisks denote corresponding parameters in the critical point of the $P_s(L)$ dependence. Note that in both instruments, MPT2 and BPA-1, use is made of this detail. Therefore, the dead time in the critical point t_d* (shown by an arrow in Fig. 7) for the capillary employed is 11.0 and 11.5 ms for water and C_{12}DMPO solution, respectively. The lines, calculated from Eq. (5), agree satisfactorily with the measured values. At the same time, the results indicate that the minimum dead time measured from flow oscillations in the BPA (i.e. the t_d* value in the critical point in the $P_s(L)$ dependence) is approximately 1 ms lower than that calculated from the assumption that V_s = constant. For the two liquids (water and C_{12}DMPO solution) this value is 10.0 ms. This difference results from the hydrodynamic effects occurring at high bubble formation frequencies and is considered only in the measurement procedure of the BPA [53]. As the lifetime in the critical point is taken to be zero, this error in the determination of the dead time would lead to a larger relative error in t_l and amounts to approximately 10% in the millisecond time range [2]. The absolute error in the determination of $t_l > 20$ ms would also be higher; however, the relative error in the t_l time range 20–100 ms would not exceed 10%, and decreases with increasing t_b down to 5%. Thus, the explicit lifetime measurement via flow oscillations decreases the standard error of t_l measurements to half as compared with other procedures.

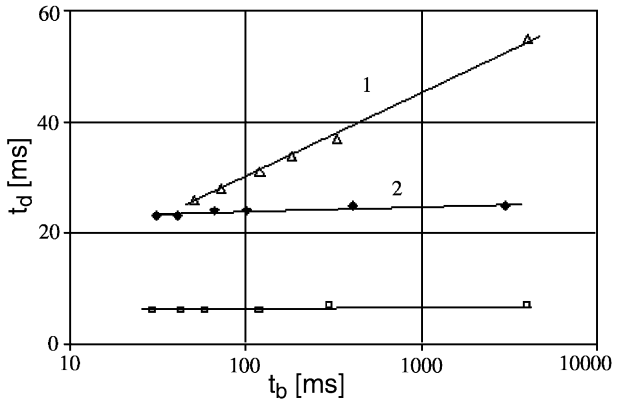

Fig. 8. The same as in Fig. 7 for V_s = 20.5 ml and (□) the capillary radius 0.125 mm, water; (♦) the capillary radius 0.075 mm, water; (△) the capillary radius 0.075 mm, C_{12}DMPO solution.

It follows from the theory [2,7] that for a fixed bubble volume any increase in the capillary radius results in a decrease of the dead time t_d, and vice versa. Results of studies performed for capillaries of radii 0.075 and 0.125 mm, respectively, are shown in Fig. 8 and exhibit good agreement with the theory [2,7]. In both cases the capillary length was 10 mm and the volume of the bubbles 2–3 mm^3. The lines in this figure were calculated from Eq. (5).

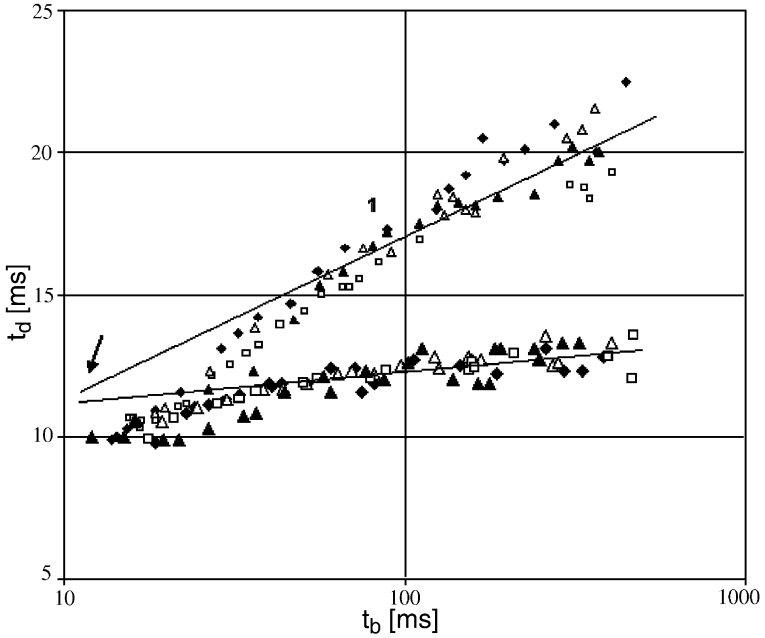

Fig. 7. The dependence of the dead time t_d on the bubble time $t_b = t_d + t_l$ for water (below) and C_{12}DMPO solution (above) for the capillary radius 0.085 mm and measuring system volume V_s = 1.5 (♦), 3.7 (□), 4.5 (△) and 20.5 ml (▲). Straight lines 1 (C_{12}DMPO solution) and 2 (water) were calculated from Eq. (5).

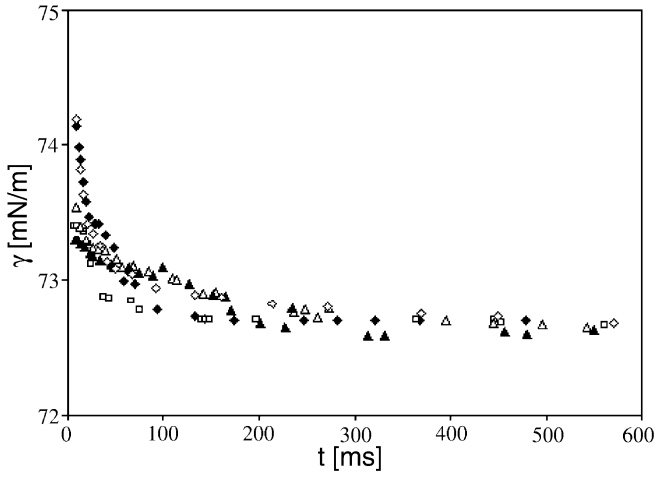

Fig. 9. The dependence of apparent dynamic surface tension of water at 20 °C and measuring system volume $V_s = 1.5$ (♦), 3.7 (□), 4.5 (△) and 20.5 ml (▲). (◇) The results obtained with capillary radius 0.125 mm and $V_s = 4$ ml.

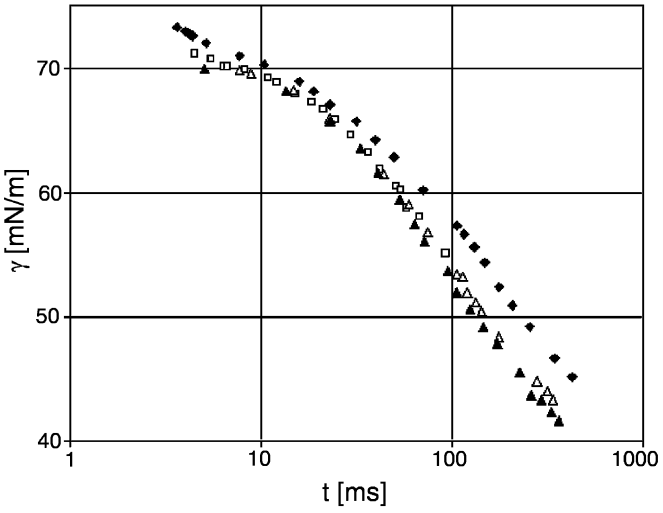

Fig. 10. The dependence of measured dynamic surface tension of C_{12}DMPO solution at 20 °C and measuring system volume $V_s = 1.5$ (♦), 3.7 (□), 4.5 (△) and 20.5 ml (▲).

3.3. Effect of the system volume V_s on measured dynamic surface tensions

The apparent dynamic surface tensions of water at 20 °C for various volumes of the measuring system are shown in Fig. 9 (data from the tensiometer BPA-1 [53]). To eliminate errors caused by an incorrect capillary radius and bubble non-sphericity, a calibration with respect to water can be performed, using the known reference surface tension (72.75 mN/m at 20 °C).

In the tensiometer MPT2 the calibration is performed in the surface lifetime range of 0.3–0.6 s, in order to eliminate additional dynamic effects [2,21–27]. One can see that in the surface lifetime beyond 300 ms, the measurement results made for different system volumes reproduce the reference value for water within 0.1 mN/m. In the BPA, the calibration is performed in a similar time range (0.5–1 s). To eliminate aerodynamic resistance effects, the dependence of excess surface tension correction term $\Delta\gamma_a(t_l)$ in the range $t_l < 1$ s is approximated by a fourth order polynomial.

In the range $t_l < 100$ ms the measured (apparent) surface tension is higher than the reference value. This is due to the hydrodynamic effects caused by the rapid bubble growth and has to be corrected [2]. It should be noted that for a small system volume ($V_s = 1.5$ cm^3) the increase in the apparent surface tension value is significantly higher. This additional effect is predicted by the theory [7,30] where the use of small volume reservoirs is considered.

The effect of the system volume V_s on the dynamic surface tension of C_{12}DMPO solutions is illustrated in

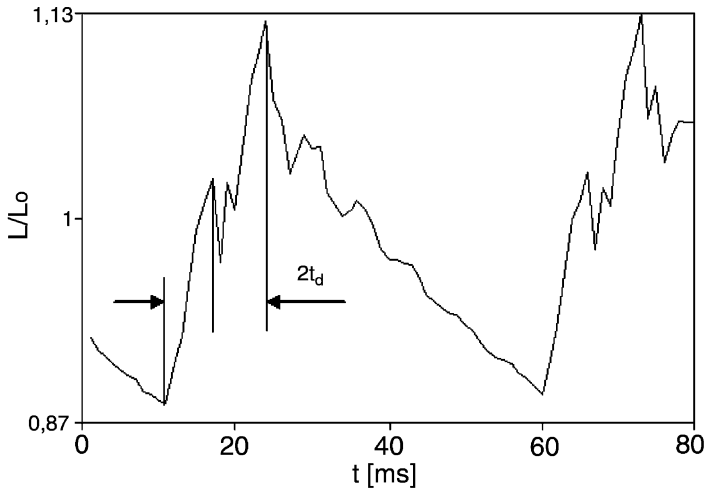

Fig. 11. Example of the series consisting of two bubbles detected from the flow oscillations.

Fig. 10. The results are in agreement with the predictions of the theoretical model [7,30]: the lower the system volume, the higher is the apparent dynamic surface tension in the millisecond time range, because an excess pressure in the system is needed to generate bubbles at a given frequency. Only at very long times (10 s and more; not shown in Fig. 10), i.e. in the vicinity of equilibrium, one can expect overlap of all dependencies for different system volumes. We can see that for a system volume $V_s = 1.5$ cm^3 the error in the measured γ values, as compared with the value for $V_s = 20.5$ cm^3, is between 5 and 10%. At the same time, the error in the dynamic surface tensions measurement for $V_s = 20.5$ cm^3 are only 1–2% lower than those for $V_s = 4.5$ cm^3.

3.4. Optimisation of the system volume

On the basis of the results in the previous sections we can make a rational choice of the measuring system volume, which ensures precise measurement of both the lifetime and surface tension. Clearly, systems with a volume less than 4 ml (i.e. $V_s/V_b < 2.000$) cannot ensure a precise measurement of the maximum pressure (i.e. surface tension) sufficient for scientific investigations and most technologic purposes. Therefore, to increase the measurement accuracy one should employ systems with larger gas volume. On the other hand, if the system volume is very high (say, $V_s/V_b > 10.000$), undesirable hydrodynamic effects and technical problems arise. One of the major negative effects for large V_s is the formation of bubble series [7]. If the pressure drop ΔP_s in the measuring system during the separation of a bubble is too small, then the inertia of the gas can generate the formation of series of two or more bubbles. This bubble series formation is known to introduce significant errors in the determination of surface tension and lifetime. The results of measurements for a capillary of radius 0.125 mm, immersed into water, and a system volume approximately 40 cm^3, are shown in Fig. 11. The formation of series of two subsequent bubbles is clearly visible. Another drawback related to systems of very large volume is the increased pressure relaxation time in the system following a flow rate variation. For example, a system of 40 cm^3 volume requires 15–20 s for pressure stabilisation after a change of the flow rate. This makes the measurement procedure more time consuming. Also, much more foam could be formed in such cases, which prevents the use of the method for small sample volumes, e.g. in medical applications [50].

Therefore, the optimum system volume, if all factors are taken into account, is that yielding a ratio of V_s/V_b in the range between 2.000 and 5000. As for such volumes the use of pressure oscillations for the determination of lifetime has large errors, gas flow oscillations are superior and should be analysed instead [53].

3.5. Determination of the hydrodynamic pressure

Simon [1] used a single capillary in his experiment and therefore the immersion depth of the capillary into the liquid had to be measured to account for the hydrostatic pressure. This depth would not have to be measured if the capillary tip is exactly at the liquid level [8] or if two capillaries (narrow and wide) are used, as proposed by Sugden [9]. This idea was further developed by other authors leading to various modifications of the MBP method, based on the measurement of the immersion depth difference for capillaries with different diameters in the same liquid, of two identical capillaries in different liquids, etc. [10–15]. Due to our opinion, setups with two capillaries can be successfully used in studies only of pure liquids or highly concentrated solutions (cf., for example, Refs. [16,17]). For usual surfactant solutions, however, due to the dynamic char-

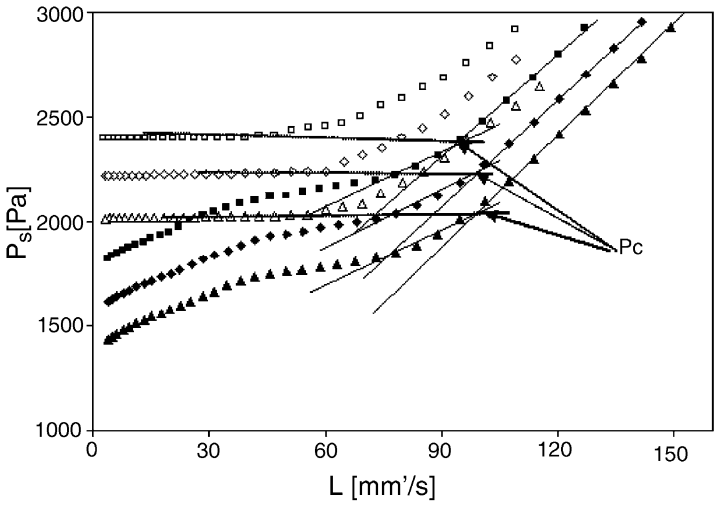

Fig. 12. The dependence of the pressure in the measuring system of the tensiometer MPT2 on the flow rate for water (□, ◇, △) and C_{12}DMPO solution (■, ♦, ▲) for the hydrostatic pressure values 100 (△, ▲), 300 (◇, ♦) and 500 Pa (□, ■).

acter of the surface tension, significant errors can arise caused by the fact that surface tensions in bubbles of different size are different. It is very difficult to satisfy the condition $\gamma = \text{constant}$, because it is insufficient to ensure equal lifetimes for the two compared bubbles. Moreover, although it is difficult to enforce equal dead times for both capillaries, this does not necessarily ensure equal initial surfactant load on the surface of small and large bubbles [30].

An approximation of the hydrostatic pressure, without any measurements of the capillary immersion depth, can be performed using a single capillary. Such a procedure is implemented, for example, in the tensiometer T60 [54,55]: a low V_s/V_b ratio and a large radius of the separating bubble ensure that the pressure in the minimum point of the $P_s(t)$ curve is approximately equal to the hydrostatic pressure. In the MPT2 tensiometer the existing procedure of determination of the critical point in the $P_s(L)$ dependence can be used for the correction of the hydrostatic pressure. Examples of such dependencies for water and a C_{12}DMPO solution, obtained for various values of the hydrostatic pressure (100–500 Pa), are shown in Fig. 12. One can see that the critical pressure P_c (shown by arrows) for any given hydrostatic pressure in the case of C_{12}DMPO solution is exactly equal to the pressure in the measuring system throughout the whole range of the bubble regime ($P < P_c$) for water with the same hydrostatic pressure. It is seen from the dependencies presented in Fig. 12 that the hydrostatic pressure determined in this way differs from the value measured from the capillary immersion depth by less than 20 Pa. Obviously, the accuracy of the P_H calculation with this method depends on the accuracy of the determination of P_c. For diluted solutions, where the slope of the P_s vs. L curve at $P < P_c$ changes significantly, such problem does not exist. For higher concentrated solutions (cf. Fig. 12) one can improve the accuracy of the determination of P_c, analysing gas flow oscillations. When the critical pressure (i.e. from single bubble to the gas jet regime) is passed, a sharp decrease is observed in the oscillation amplitude, and the flow oscillations become irregular: the standard deviation of the determination of t_b becomes 100% and more, instead of 10–15%. In addition to the correction of the hydrostatic pressure, this method allows to compensate small excess pressure caused by other reasons.

However, to perform precise measurements of dynamic surface tension, one should account for the hydrostatic pressure by accurate measurements of the capillary immersion depth. It should be noted that for narrow capillaries an even rather low accuracy of this procedure (say, to within 0.3 mm) results in surface tension errors less than 0.5%.

In the BPA-1 single capillaries are employed. To exactly account for the hydrostatic pressure P_H, the liquid/gas interface is automatically determined via the pressure jump appearing when the capillary touches the liquid surface. Subsequently, the capillary is immersed into the liquid to a depth chosen by the user (2–20 mm, with an accuracy of ± 0.05 mm).

3.6. Dynamic surface tensions at longer adsorption times

It was noted above that during the separation of a bubble the pressure in the measuring system decreases by ΔP_s (Eq. (4)). For relatively large system volumes, this phenomenon leads to a self-generation of bubbles with longer lifetimes. This method, the so-called stopped flow method, is implemented in the MPT2 tensiometer [2]. If the system is absolutely hermetic, then the surface

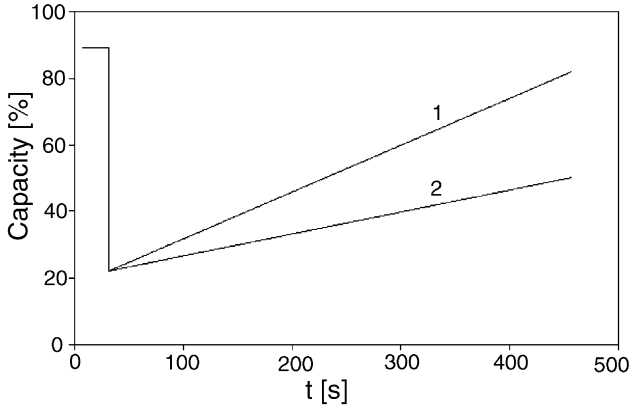

Fig. 13. Examples showing the time dependence of the relative power supplied to the Peltier generator.

tension change per separating bubble is given by [2]

$$\Delta\gamma = \frac{r(P_a + P_s)V_b}{2V_s}. \quad (6)$$

Therefore, increasing time intervals between separating bubbles result, depending on the rate of surface tension decrease. The lifetime of each subsequent bubble is higher than that of the preceding one. However, this method is characterised by some deficiencies. First, to implement this method, the measuring system volume should be comparatively large. Best results were obtained for 100–500 cm^3 [2]. However, it was shown above that for large system volumes the bubble series can appear. In addition, small air leakage through valves and small temperature changes in the system by the thermostatic control restrict a controlled generation of bubbles to times of approximately 10 s, especially when γ changes only slightly with time.

To extend the region, in which the bubble lifetime can be measured, tensiometers can be equipped with a Peltier bubble generator (up to 100 s in the tensiometers MPT2 and BPA) [53]. The generator 9 is connected to the volume 8 (Fig. 1) and controlled by the computer 13 via the interface 12. Before the generator is started, the initial bubble interval of approximately 0.5 s is set up by the compressor 1. Then the compressor is cut off the measuring system by the valve 10 (cf. Fig. 1), and in the same moment the Peltier generator is activated. The design of the generator with an internal volume of approximately 3 cm^3 allows the generation of 100 bubbles via heating of the Peltier elements to its maximum temperature over a time interval of 3–30 min. The optimal regime for the power change supplied to the generator was optimised experimentally so that the interval between bubbles is gradually increased, and, at the same time, the surface tension of the studied solution for consecutive bubbles decreases. Two examples of power regimes for the Peltier generator are shown in Fig. 13. Typically, the power is maximal during the first 10–30 s, ensuring an initial generation of bubbles with intervals of 0.5 to 2–3 s. Then the power is sharply decreased to 20–50% of the maximum value, and a regime of slow linear power increase up to the maximum value follows for a fixed duration of the experimental run. For a slow surface tension decrease the rapid regime is preferred (line 1), while for a faster surface tension decrease the slower heating regime is suitable (line 2). Examples obtained in studies of biologic liquids (using regime 2) are shown in Fig. 14. The total volume of the measuring system and the Peltier elements in these experiments was 25 cm^3. For comparison, the dependencies obtained for the same liquids without the Peltier generator, i.e. measured with the stopped flow procedure, are also presented as solid symbols in Fig. 14. For $t > 1$ s and the stopped flow regime only a few points are obtained, insufficient for an analysis of a $\gamma(t)$ dependence in the long time range [50].

After the experimental run is completed, the Peltier elements are cooled down by applying the inversed electric current. This option can be used also to increase the number of generated bubbles—in this case the Peltier elements should be preliminary cooled.

3.7. Dependence of dead time on the geometry of the capillary

The dead time t_d in the critical point is determined from the relationship $t_d = V_b/L_c$, where L_c is the gas flow at the critical point [2]. For any system pressure (and any gas flow), a correction to the dead time can be introduced using Eq. (5). In turn, the critical flow is determined by the capillary parameters [2], i.e. the longer the capillary and the smaller its diameter, the

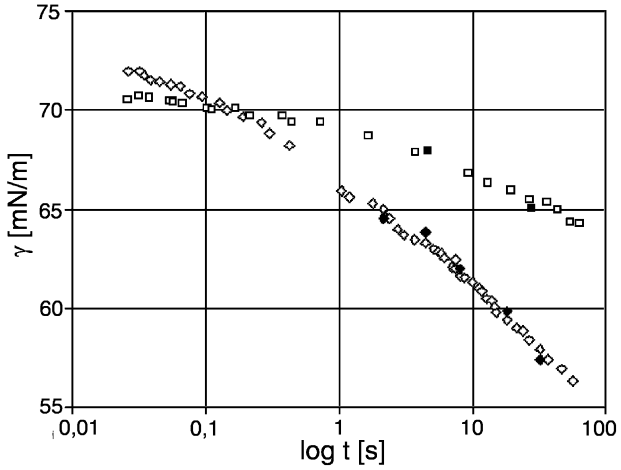

Fig. 14. The dependence of dynamic surface tension for cerebrospinal fluid (□, ■) and blood serum (◇, ◆) with the Peltier generator activated (□, ◇) and not activated (■, ◆).

lower is the gas flow in the critical point. Therefore, for a fixed capillary radius one can control the critical gas flow rate L_c (and, therefore, the dead time) by varying the capillary length [56]. However, for wide capillaries (diameter $2r \geqslant 0.25$ mm) the respective capillary length can be quite long, so that this procedure becomes impracticable for the control of the critical flow. This obstacle could be overcome by using combined narrow and wide capillaries, arranged by a wide capillary immersed into the liquid and connected to a narrow capillary, or by decreasing the cross-section of a wide capillary in its upper part by a special insert. Note that these methods could be used to control the dead time only in systems for which the condition $V_b \ll V_s(P_s/P_a)$ is fulfilled (P_a is the atmospheric pressure). This condition corresponds to the situation when the gas mass excess in the system is large enough to enable a spontaneous formation of bubbles during the dead time, controlled only by the capillary resistance. However, in some devices this condition does not hold, and therefore the dead time varies quite strongly, because the process of bubble growth is determined by the gas flow from the compressor to the measuring system [54,55,57].

From the theory for the MBPM the critical gas flow L_c can be readily calculated from the aerodynamic resistance of the capillary [2]. The following relationship for a capillary with arbitrary geometry follows from the Poiseuille law ([2], Eq. (15)):

$$\frac{P_c}{L_c k_P} = \text{constant} = K, \tag{7}$$

$k_P = 8\eta l/\pi r^4$ is the Poiseuille coefficient that depends on the gas viscosity η, the capillary length l and radius r. The coefficient k_P can be determined experimentally when the capillary is not immersed into the liquid and we get $k_P = dP/dL$. The theoretical value of the dimensionless constant $K > 1$ is in agreement with experimental findings ($K \cong 1.6$) [2].

As the dead time is determined by V_b and L_c, it is possible to control t_d for any capillary diameter. This can be achieved by varying the critical flow rate L_c that depends on the aerodynamic resistance of the capillary (Eq. (3)), and also by the value of V_b that in turn depends on the position of the bubble deflector. Note that the shorter the dead time, the lower is the initial adsorption at the bubble surface, and consequently the lower is the surface lifetimes available for the studies [2,58].

It was demonstrated experimentally that, under equal conditions (capillary diameter, surface tension), an elongation of the capillary, the introduction of an additional resistance and smaller bubble volumes V_b lower the value for L_c. In contrast to static conditions, i.e. when bubbles separate due to buoyancy force, under dynamic conditions the pressure exerted onto the bubble by the gas inflow from the capillary plays a significant role. In this case, the higher the pressure created by the gas flow, the smaller is the bubble size. However, if the gas flow velocity is too high, the bubble can exceed a critical size, determined by the balance between buoyancy and capillary forces. For water and a capillary diameter of 0.25 mm this critical size is 5.7 mm^3. This is caused by the continuous gas inflow into the bubble from the measuring system during the separation of the bubble from the capillary. These opposite trends in the bubble volume caused by the increase in the gas flow velocity was recently studied experimentally [56]. For example, with a capillary diameter of 0.25 mm and length of 15 mm, which refers to a high velocity of the gas flow from the capillary, we obtain $L_c = 300$ mm^3/s and $V_b = 10$ mm^3. This is approximately two times higher than the critical size. For a capillary with the same diameter and 57-mm length, the gas velocity is four times lower and values of $L_c = 83$ mm^3/s and $V_b = 2.75$ mm^3 were obtained. These values are approximately two times lower than the critical size determined from the balance between buoyancy and capillary forces. These two capillaries are characterised by approximately the same dead time of $t_d = 30–35$ ms. Therefore, the capillary with high aerodynamic resistance can be used without a bubble deflector and would be convenient in measurements with foam-forming low concentrated solutions, and at lifetimes larger than 5 ms. On the contrary, a shorter capillary but with bubble deflector (in this case V_b can be obtained as small as 2 mm^3) can be employed in studies of concentrated solutions and surface lifetimes below 1 ms, because the corresponding dead time is as low as 5 ms [2,57]. In summary, the variation of the capillary geometry can help to achieve optimum characteristics of the bubble formation process, such as critical gas flow, bubble volume and dead time.

3.8. Correction of a non-spherical bubble shape

As mentioned above, when capillaries of larger diameter are used, the shape of the generated bubbles is not ideally spherical. Thus, using the capillary radius r_{cap} as radius of curvature for the calculation of the capillary pressure leads to significant errors. The larger the capillary is, the more significant are the deviations from sphericity and hence the resulting errors.

The BPA can employ capillaries of diameter between 0.25 and 1.0 mm, and the surface tension is calculated with an automatic correction for the non-sphericity of the bubble. The correction factor (Eq. (3)) is given by [2]

$$f = \sum a_i \left(\frac{r}{a}\right)^i, \tag{8}$$

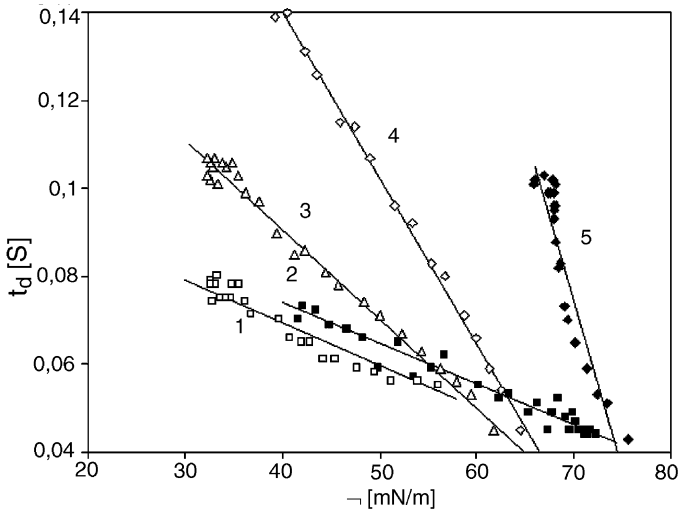

Fig. 15. Dead time as a function of surface tension for the Triton X-100 (2 mmol/l) and $C_{12}EO_6$ (0.3 mmol/l) aqueous solutions (curves 1 and 2, respectively); the Triton X-100 (2 mmol/l) solutions in 50 and 70% solutions of glycerine in water (curves 3 and 4, respectively), and 80% glycerine aqueous solution (curve 5); the viscosity values were 1 mm^2/s (solutions 1 and 2), 5, 23 and 52 mm^2/s (solutions 3, 4 and 5).

where a is the capillary constant defined by

$$a=\sqrt{\frac{2\gamma}{\Delta\rho g}}, \tag{9}$$

and the coefficients in Eq. (8) have the following values [35]: $a_0=0.99951$, $a_1=0.01359$, $a_2=-0.69498$, $a_3=-0.11133$, $a_4=0.56447$, $a_5=-0.20156$.

3.9. Influence of the liquid viscosity on surface tension measurements

The tensiometers MPT2 and BPA have options to introduce a correction for the viscosity of the studied liquid. The viscosity is considered to be known for the studied system. In this case, the BPA measuring program, for example, employs a procedure that accounts for an additional resistance at short bubble lifetimes (Eq. (3)) as [2]

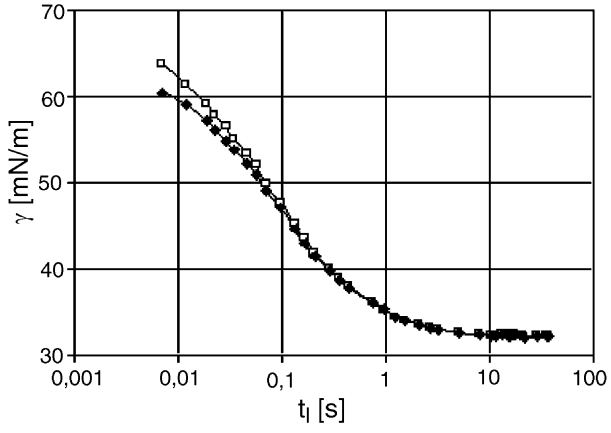

Fig. 16. Non-corrected (open circles) and corrected (filled circles) dependences of the surface tension for 2 mmol/l Triton X-100 in a 50% glycerine solution.

$$\Delta\gamma_v=(-\Psi-\phi\ln t_l)\frac{P}{P_{cal}}\ln\eta. \tag{10}$$

where Ψ and ϕ are constants, t_l is the measured lifetime, P is the actual pressure, P_{cal} is the calibration pressure for water and η is the viscosity of the liquid. An additional procedure is implemented, on the basis of a correlation between the viscosity and the dead time values [59]

$$t_d=A-\alpha\gamma \tag{11}$$

where A and α are constants characteristic for each liquid. It is important that the slope of the t_d vs. surface tension curve depends on the viscosity of the liquid. Some examples of such dependencies are shown in Fig. 15. The higher the liquid viscosity, the larger is the slope of the dependence $t_d(\gamma)$. This fact can be explained by an increasing bubble volume separating from the capillary, because the increase in viscosity leads to a retardation of the bubble separation process. For viscosities $2\ mm^2/s<\eta<100\ mm^2/s$, the dependence of α on η is quite linear. Therefore, we obtain

$$\alpha=B+\beta\eta \tag{12}$$

where B and β are constants. If the viscosity is in the given range, the user does not need to input the viscosity value along with other parameters of the studied system because the software determines it. As an example, non-

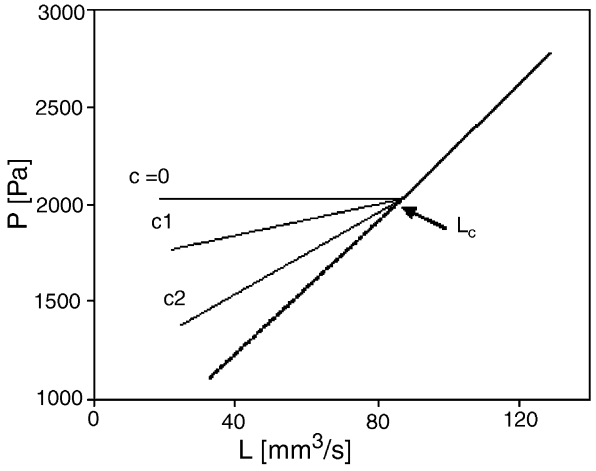

Fig. 17. Schematic dependence of pressure in the measuring system on the gas flow through the capillary for pure water ($c=0$) and surfactant solutions of concentrations $c_1<c_2$.

corrected (open circles) and corrected (filled circles) surface tensions for a 2 mmol/l Triton X-100 in a 50% glycerine solution are shown in Fig. 16. The viscosity obtained from Eq. (12) is $\eta=6.1$ mm^2/s, instead of 6.3 mm^2/s measured directly for the water/glycerine mixture. Both effects, $\Delta\gamma_a$ and $\Delta\gamma_v$ (Eq. (3)), fade out at lifetimes $t_l>0.5$ s.

3.10. Limits of applicability of the maximum bubble pressure method

The time range available for an MBP instrument for measuring dynamic surface tensions is mainly determined by the capillary parameters and the size of the separating bubble. The dependence of the excess pressure P_s on the gas flow L two regimes lets us distinguish (cf. Fig. 17) the gas jet flow regime for flow rates above the critical value L_c (indicated by an arrow), and the single bubble regime for $L<L_c$. In the critical point bubbles are formed continuously and the interval between bubbles t_b is exactly equal to the dead time t_d. The slope of the line in the jet regime range is determined by the aerodynamic resistance of the capillary k_P [2]:

$$\frac{dP_s}{dL}=k_P\equiv\frac{8\eta l}{\pi r^4}. \tag{13}$$

The dependence of P_s on L for any solvent ($c=0$) in the bubble regime region is parallel to the abscissa axis. The higher is the surfactant concentration in the solution ($c_2>c_1$), the higher is the slope of the dependence $P_s(L)$ in the region $L<L_c$. Clearly, the slope cannot exceed k_P, because the gas flow velocity along the capillary cannot exceed that predicted by the Poiseuille law (Eq. (13)). Therefore, expressing the kinetics of adsorption at a growing bubble via the derivative dP_s/dL, one can determine the values of the capillary parameters for which the surface tension γ of a given solution could be studied. The excess pressure in the system can be expressed approximately (Eq. (1)) by $P_s=2\gamma/r$, while the air flow in the capillary can be approximated by $L=V_b/t_b$ using the bubble volume V_b and the bubble time t_b. The derivative dP_s/dL ($V_b=$constant and $t_d=$ constant) caused by adsorption (index a) is given by

$$\left(\frac{dP_s}{dL}\right)_a=-\frac{2t_b^2}{rV_b}\left(\frac{d\gamma}{dt_l}\right)=\frac{2t_b^2}{rV_b}\left(\frac{d\Pi}{dt_l}\right), \tag{14}$$

where $\Pi=\gamma_0-\gamma$ is the surface pressure of the surfactant solution and γ_0 is the surface tension of the pure solvent. As mentioned above, the relation between any derivatives dP_s/dL and $(dP_s/dL)_a$ holds

$$\frac{dP_s}{dL}\geqslant\left(\frac{dP_s}{dL}\right)_a \tag{15}$$

which, together with Eq. (14), yields the requirement for $(d\Pi/dt_l)_a$ for a studied solution:

$$\left(\frac{d\Pi}{dt_l}\right)_a\leqslant\frac{k_P r V_b}{2t_b^2} \tag{16}$$

Therefore, only capillaries with high enough aerodynamic resistance (the constant k_P) can be used to analyse the adsorption processes characterised by high values of the derivative $(d\Pi/dt_l)_a$. Eq. (16) can be specified if we assume a diffusion controlled adsorption kinetics for the surfactant and use the approximation for the dead time derived in Ref. [60]. For short lifetimes, $t_d\gg t_l$, a criterion was derived in Ref. [56], which allows to estimate the potential capacity of an MBPM:

$$\left(\frac{d\Pi}{dt_l}\right)_a\leqslant\frac{\gamma_0 t_d}{1.6(t_l+t_d)^2}. \tag{17}$$

For a diffusion controlled adsorption mechanism and a capillary with $t_d=100$ ms, solutions with concentrations $c<1$ mmol/l can be studied in a time interval $t_l>3$ ms. If we use, however, a capillary with $t_d=10$ ms, we can investigate solutions up to concentration of 5 mmol/l [56]. Clearly, these estimates are only the lower concentration limits, especially when the adsorption mechanism is not based on diffusional transport. For micellar solutions and solutions of ionic surfactants, the adsorption rate is lower than predicted by the diffusion model [5]. Therefore, the MBPM can usually be applied to higher concentrations.

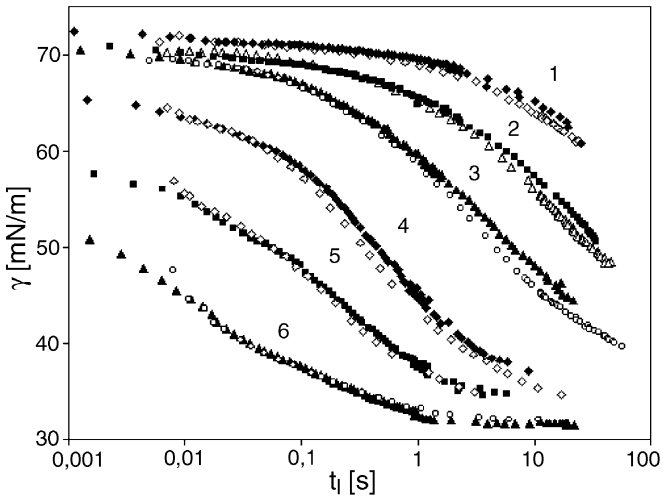

Fig. 18. The dependence of dynamic surface tension of Triton X-100 solution at temperature 22–23 °C for different concentration: 0.05 (curve 1), 0.1 (curve 2), 0.2 (curve 3), 0.5 (curve 4), 1.0 (curve 5) and 2.0 mmol/l (curve 6); open symbols—BPA, closed symbols—MPT2.

3.11. Comparison of dynamic surface tensions measured by different MBP tensiometers

It is interesting to compare the results obtained for the same surfactant solution but with different instruments. We present here measurement for Triton X-100 solutions using MPT2 (detection of t_b and recalculation of t_l via the critical point in the $P(L)$ dependence) and BPA (direct detection of t_l via the gas flow oscillations $L(t)$), and discuss the discrepancies between the observed results.

Fig. 18 gives the dynamic surface tensions measured for various Triton X-100 concentrations. The γ values obtained with the tensiometer MPT2 having a system volume of approximately 40 ml and a capillary of radius $r=0.125$ mm are in a good agreement with the data obtained by the BPA having a system volume $V_s=4.5$ ml and a capillary of radius $r=0.125$ mm.

It was shown in Ref. [51] that $\gamma(t)$ values obtained with the SITA tensiometer T60 are essentially lower than those measured by the Krüss tensiometer BP2, and data of both are lower than those measured with the MPT2 and BPA tensiometers. We believe that the inconsistency between the results obtained by various devices is mainly caused by the differences in the geometric characteristics of the capillaries and measuring systems, which leads to differences in the dead time and, hence, in the bubble volume.

4. Conclusions

Significant progress was made in maximum bubble pressure tensiometry in the millisecond time range. This progress is based on the analysis of gas flow rather than pressure oscillations in the measuring system to be used to determine the duration of all phases of bubble formation. The design and operational principles of different MBP tensiometers are described here, and the influence of the main parameters of the measuring system (capillary radius, measuring system volume and V_s/V_b ratio) on the measurement precision of the bubble lifetime and dynamic surface tension is analysed. In all cases, the optimum procedure found is to employ sufficiently narrow capillaries (with radius not exceeding 0.15 mm) and measuring systems with a ratio V_s/V_b in the range between 2.000 and 5.000. The errors arising for wide capillaries (radius up to 1 mm) and by lifetime measurements via pressure oscillations are examined. It is shown that wide capillaries are not acceptable due to uncontrolled errors in the dynamic surface tension measurements (of the order of 10% and more). Time detection via pressure oscillations, for narrow capillaries, provides quite acceptable surface tension results for technical applications (accuracy within 5%) in a surface lifetime range $t_l \geqslant 10$ ms. The analysis of various methods used to account for the hydrostatic pressure (two capillaries method, minimum system pressure method or jet regime critical pressure shift method) shows that for studies of surfactant solutions with narrow capillaries best results can be obtained when the capillary immersion depth is measured directly. To study dynamic surface tensions in the time range of 0.5–100 s, a Peltier generator is advantageous.

Acknowledgments

The work was financially supported by the DFG (Mi 418/11) and the ESA project FASES MAP AO-99-052.

References

[1] M. Simon, Ann. Chim. Phys. 32 (1851) 5.
[2] V.B. Fainerman, R. Miller, The maximum bubble pressure technique, monograph in 'Drops and Bubbles in Interfacial

Science', in: D. Möbius, R. Miller (Eds.), Studies of Interface Science, vol. 6, Elsevier, Amsterdam, 1998, pp. 279–326.
[3] J. Eastoe, J.S. Dalton, Adv. Colloid Interf. Sci. 85 (2000) 103.
[4] K.J. Mysels, Colloid. Surf. 43 (1990) 241.
[5] R. Miller, P. Joos, V.B. Fainerman, Adv. Colloid Interf. Sci. 49 (1994) 249.
[6] A.I. Rusanov, V.A. Prokhorov, Interfacial tensiometry, in: D. Möbius, R. Miller (Eds.), Studies in Interface Science, vol. 3, Elsevier, Amsterdam, 1996.
[7] V.I. Kovalchuk, S.S. Dukhin, Colloid. Surf. A 192 (2001) 131.
[8] R.C. Brown, Philos. Mag. 13 (1932) 578.
[9] S. Sugden, J. Chem. Soc. 121 (1922) 858.
[10] F.M. Jaeger, K. Ned. Akad. Wet. Versl. Gewone Vergad. Atd. Natuurkd. 23 (1914) 330.
[11] F.M. Jaeger, Z. Anorg. Chem. 101 (1917) 1.
[12] E.L. Warren, Philos. Mag. 4 (1927) 358.
[13] P.P. Pugachevich, Zh. Fiz. Khim. 38 (1964) 758.
[14] P.T. Belov, Zh. Fiz. Khim. 55 (1981) 302.
[15] K. Lunkenheimer, R. Miller, J. Becht, Colloid Polym. Sci. 260 (1982) 1145.
[16] R. Razouk, D. Walmsley, J. Colloid Interf. Sci. 47 (1974) 515.
[17] J.L. Ross, W.D. Bruce, W.S. Janna, Langmuir 8 (1992) 2644.
[18] R. Miller, V.B. Fainerman, K.-H. Schano, W. Heyer, A. Hofmann, R. Hartmann, Labor Praxis, N 18 (1994) 56.
[19] E.N. Stasiuk, L.L. Schramm, Colloid Polym. Sci. 278 (2000) 1172.
[20] G. Biesmans, L. Colman, R. Vandensande, J. Colloid Interf. Sci. 199 (1998) 140.
[21] S.S. Dukhin, V.B. Fainerman, R. Miller, Colloid. Surf. A 114 (1996) 61.
[22] V.I. Kovalchuk, S.S. Dukhin, V.B. Fainerman, R. Miller, J. Colloid Interf. Sci. 197 (1998) 383.
[23] V.I. Kovalchuk, S.S. Dukhin, A.V. Makievski, V.B. Fainerman, R. Miller, J. Colloid Interf. Sci. 198 (1998) 191.
[24] S.S. Dukhin, N.A. Mishchuk, V.B. Fainerman, R. Miller, Colloid. Surf. A 138 (1998) 51.
[25] S.S. Dukhin, V.I. Kovalchuk, V.B. Fainerman, R. Miller, Colloid. Surf. A 141 (1998) 253.
[26] V.I. Kovalchuk, V.B. Fainerman, R. Miller, S.S. Dukhin, Colloid. Surf. A 143 (1998) 381.
[27] V.I. Kovalchuk, S.S. Dukhin, V.B. Fainerman, R. Miller, Colloid. Surf. A 151 (1999) 525.
[28] N.A. Mishchuk, V.B. Fainerman, V.I. Kovalchuk, R. Miller, S.S. Dukhin, Colloid. Surf. A 175 (2000) 207.
[29] S.V. Lylyk, A.V. Makievski, V.I. Kovalchuk, K.-H. Schano, V.B. Fainerman, R. Miller, Colloid. Surf. A 135 (1998) 27.
[30] N.A. Mishchuk, S.S. Dukhin, V.B. Fainerman, V.I. Kovalchuk, R. Miller, Colloid. Surf. A 192 (2001) 157.
[31] P.A. Rehbinder, Z. Phys. Chem. 111 (1924) 447.
[32] A.M. Kragh, Trans. Faraday Soc. 60 (1964) 225.
[33] M. Austin, B.B. Bright, E.A. Simpson, J. Colloid Interf. Sci. 23 (1967) 108.
[34] J. Kloubek, Tenside 5 (1968) 317.
[35] R.L. Bendure, J. Colloid Interf. Sci. 35 (1971) 238.
[36] T.E. Miller, W.C. Meyer, Am. Lab. (1984) 91.
[37] X.Y. Hua, M.J. Rosen, J. Colloid Interf. Sci. 124 (1988) 652.
[38] S.G. Woolfrey, G.M. Banzon, M.J. Groves, J. Colloid Interf. Sci. 112 (1986) 583.
[39] P.R. Garrett, D.R. Ward, J. Colloid Interf. Sci. 132 (1989) 475.
[40] D.E. Hirt, R.K. Prud'homme, B. Miller, L. Rebenfeld, Colloid. Surf. 44 (1990) 101.
[41] K.J. Mysels, Langmuir 2 (1986) 428.
[42] K.J. Mysels, Langmuir 5 (1989) 442.
[43] C.D. Dushkin, I.B. Ivanov, P.A. Kralchevsky, Colloid Surf. 60 (1991) 235.
[44] C.P. Hallowell, D.E. Hirt, J. Colloid Interf. Sci. 168 (1994) 281.
[45] Tz.H. Iliev, C.D. Dushkin, Colloid Polym. Sci. 270 (1992) 370.
[46] B.V. Zhmud, F. Tilberg, J. Kizling, Langmuir 16 (2000) 7685.
[47] J. Eastoe, J.S. Dalton, R.K. Heenan, Langmuir 14 (1998) 5719.
[48] E. Alami, K. Holmberg, J. Colloid Interf. Sci. 239 (2001) 230.
[49] K. Theander, R.J. Pugh, J. Colloid Interf. Sci. 239 (2001) 209.
[50] V.N. Kazakov, O.V. Sinyachenko, V.B. Fainerman, U. Pison, R. Miller, Dynamic surface tension of biological liquids in medicine, in: D. Möbius, R. Miller (Eds.), Studies in Interface Science, vol. 8, Elsevier, Amsterdam, 2000.
[51] J. Meissner, J. Krägel, C. Frese, S. Rupert, V.B. Fainerman, A.V. Makievski, R. Miller, Seifen-Fette-Öle-Wachse (2003) 60.
[52] V.B. Fainerman, R. Miller, A.V. Makievski, Rev. Sci. Instruments (2004) in press.
[53] R. Miller, A.V. Makievski and V.B. Fainerman, Labor Praxis (2004) in press.
[54] Patent DE 197 55 291 C1, 1997.
[55] Patent DE 199 33 631 A1, 1999.
[56] V.B. Fainerman, S.V. Lylyk, A.V. Makievski, R. Miller, Maximum bubble pressure technique to measure dynamic surface tensions of surfactant solutions in the short time range-limits of applicability, Colloid. Surf. A, submitted for publication.
[57] H. Nakae, T. Fukui, Mater. Trans. 42 (2001) 2422.
[58] V.B. Fainerman, R. Miller, J. Colloid Interf. Sci. 175 (1995) 118.
[59] V.B. Fainerman, V.D. Mys, A.V. Makievski, R. Miller, Correction for the aerodynamic resistance and viscosity in maximum bubble pressure tensiometry, Langmuir (2004) in press.
[60] V.B. Fainerman, Kolloid. Zh. 41 (1979) 111, in Russian.